JOURNAL OF APPLIED ELECTROCHEMISTRY 18 (1988) 653–656

Corrosion of stainless steel (AISI 316) in molten sodium polysulphide under applied potential

REINHARD KNÖDLER

ASEA BROWN BOVERI, Corporate Research, Heidelberg, FRG

Received 14 December 1987; revised 12 February 1988

The corrosion of AISI 316 steel has been investigated in sodium polysulphide melts in the region between 300 and 410° C which is of interest with respect to the Na/S battery. Although AISI 316 is not suitable as a corrosion-resistant casing material, it can serve as a model material for the elucidation of basic mechanisms. Both anodic and cathodic potentials were applied in order to represent the conditions in a cell. The corrosion products formed multilayer scales, the inner one consisting primarily of chromium sulphide which acted as a corrosion barrier. The corrosion reaction had an activation energy of 105 kJ mol^{-1}. In the higher temperature region the scale dissolved partially in the melt due to a change in the scale morphology. Possible mechanisms for anodic and cathodic corrosion reactions are discussed.

1. Introduction

Molten sodium polysulphides Na_2S_x with x from 3 to about 20, are used in the cathode compartment of sodium–sulphur cells. The container of these cells must be electrically conductive and corrosion resistant with respect to Na_2S_x at the operating temperature of about 350° C. There are candidate materials for such a casing, e.g. chromized steel, superalloys or inorganic compounds [1–10], but most have certain drawbacks. The developers of Na/S batteries presently use proprietary materials.

Testing of the candidate casing materials has so far been carried out mostly under static conditions (i.e. without applied potential). However, this has sometimes led to wrong conclusions. So aluminium, magnesium and titanium were considered to be stable, whereas in real cells they corrode considerably. Generally, the electrochemical aspects of corrosion in polysulphide melts have been somewhat neglected.

In this paper, we present some results of dynamic testing (i.e. with applied potential), with emphasis on the temperature dependence of corrosion. As 'model material', a standard stainless steel (AISI 316) was used. Although this steel cannot be used as an actual casing, it is suited for corrosion experiments because of its relatively large corrosion rates. Also, AISI 316 can serve as a basis for the development of more suitable alloys.

2. Experimental details

In previous investigations on the reaction mechanisms in molten polysulphides, very pure sodium polysulphide was prepared *in situ* by the electrochemical reaction between sodium and sulphur [11, 12]. However, in preliminary corrosion experiments it turned out that for this purpose there is no need for such a high-purity material. Therefore, commercially available Na_2S_4 (Degussa, Knapsack, FRG) was used. The electrochemical cell consisted of a glass tube with the working electrode and the counter electrode of the same material for which the corrosion rate was to be measured. Thus, in a single experiment, both anodic and cathodic rates could be determined. The reference electrode consisted of a graphite rod which shows sufficient stability. The cell was sealed with Viton gaskets (in the colder region of the furnace) and was operated in a glove box, flushed with nitrogen.

The test specimens were rods of 5 mm diameter and about 35 mm length. They were positioned about 15 mm deep in the melt, exhibiting a surface area of about 2 cm^2 to corrosion attack. Prior to insertion into the melt, the specimens were polished to about 1 μm. This appears satisfactory regarding the uniformness of diameter. The composition, as measured by X-ray fluorescence analysis was 10% Ni, 16.5% Cr, 2% Mo, 1% Si, 2% Mn, bal. Fe. This is a 1.4571 (German) steel, corresponding to AISI 316 (US).

The specimens were charged by a constant anodic or cathodic current of 100 mA cm^{-2} which corresponds to the values in a real Na/S cell. The anodic (purely ohmic) overpotential was about 300 mV with respect to the reference electrode, while the cathodic values scattered between -1.8 and -2.2 V. The anodic process is the oxidation of Na_2S_4 to sulphur, the cathodic process the reduction of Na_2S_4 to Na_2S_2. Because Na_2S_2 forms a solid film on the electrode, the overpotential shows relatively high values [11]. Compared to the relatively high redox currents, the superimposed corrosion currents, which are in the range of a few μA cm^{-2}, could not be measured separately. During operation, the overall melt composition remained unchanged.

After an operation time of 500 h the specimens were removed from the melt and rinsed with distilled water. The cathodically operated specimens showed a shiny surface with no scale. A few samples were corroded

0021-891X/88 $03.00 + .12

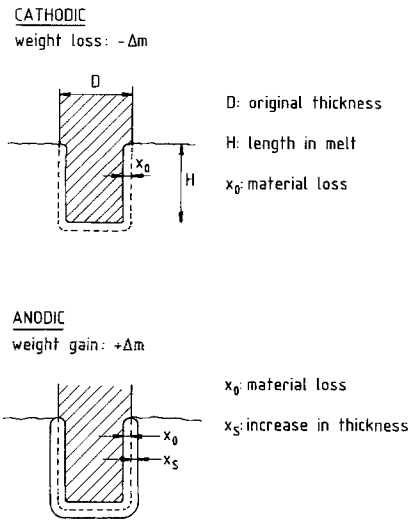

Fig. 1. Evaluation of results after cathodic and anodic operation.

also above the melt due to the melt meniscus. This effect was found mainly at higher cathodic current densities. The corrosion rate, x_0, was calculated by directly measuring the decrease in diameter and independently by determining the weight loss Δm and calculating the corrosion rate (see Fig. 1), using

$$x_0 = \frac{4\Delta m}{D\pi\delta(D + 4H)} \tag{1}$$

where δ is the density of the test material.

The anodically operated specimens showed a metal sulphide scale, resulting in a weight gain (Fig. 1). No corrosion at the melt meniscus was observed. In this case the corrosion rate, i.e. the actual material loss, was calculated as the amount of material converted to metal sulphide. By analogy to Equation 1 the material loss is

$$x_0 = \frac{4f_1\Delta m}{D\pi\delta(D + 4H)} \tag{2}$$

where $f_1 = n_m M_m / n_s M_s$, M_m and M_s being the atomic weight of metal in the alloy and of sulphur, respectively, and n_m and n_s the reaction numbers for the formation of the metal sulphide. As an average between FeS, FeS_2, Ni_2S_3 and Cr_2S_3, $f_1 \simeq 1.3$. The increase in thickness due to the scale can be calculated as

$$x_s = \frac{4\Delta m}{\pi} \cdot \frac{f_2/P - f_1/\delta}{D(D + 4H)} \tag{3}$$

where P is the porosity of the scale (100% = 1) and

$$f_2 = f_1\left(\frac{1}{\delta_s} - \frac{1}{\delta}\right) + \frac{1}{\delta_s} \tag{4}$$

where δ_s is the density of the sulphide. f_2 is the ratio of the volume increase ΔV to the mass increase Δm. The average value of f_2 for the scale sulphides is about 0.35. x_s was determined by the increase in thickness, $x_0 + x_s$ was obtained from cross sections (e.g. Figs 3 and 4) and x_0 by the weight change according to Equation 2 and, in addition, geometrically after mechanically removing the scale. Inconsistencies between these measurements indicate a loss of scale material (either by spalling or by chemical dissolution).

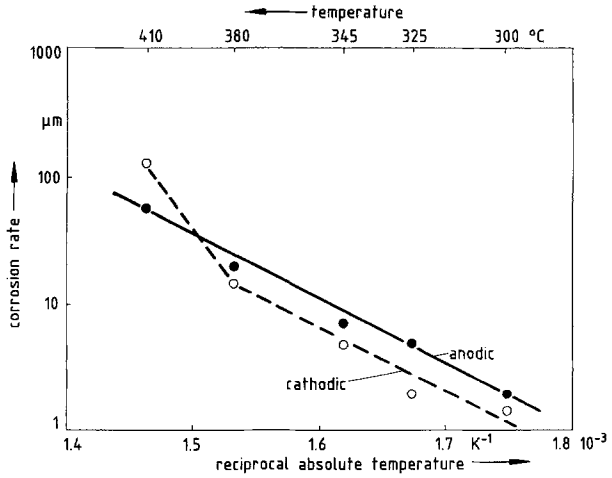

Fig. 2. Corrosion rate after 500 h operation at 100 mA cm^{-2}. Activation energy: 105 kJ mol^{-1}.

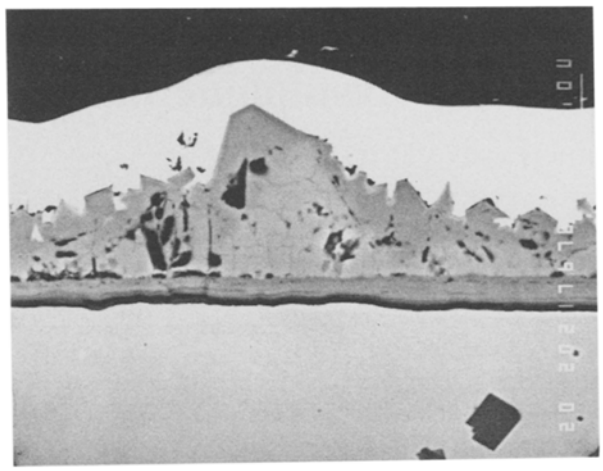

Fig. 3. Corrosion layer at 325° C (500 h anodic operation).

3. Results

The corrosion rate as a function of temperature between 300 and 410° C is shown in Fig. 2. It can be seen that the anodic corrosion under the described conditions is an activated process with an activation

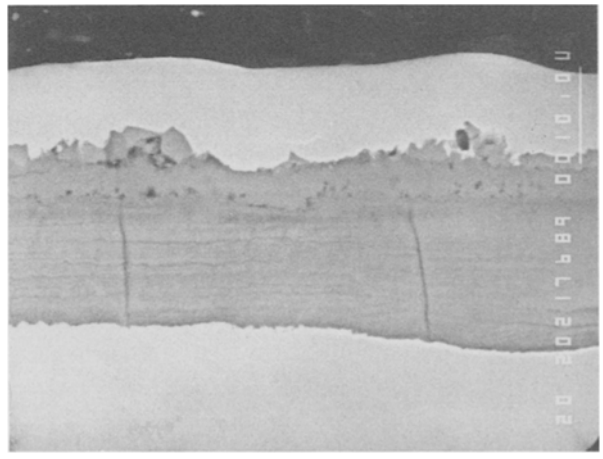

Fig. 4. Corrosion layer at 410° C (500 h anodic operation).

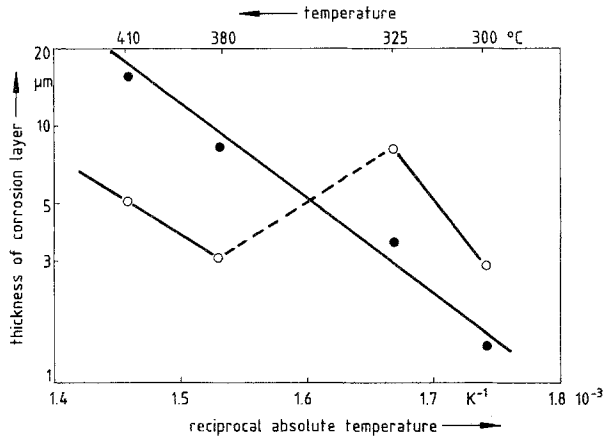

Fig. 5. Thickness of the anodic corrosion layer formed after 500 h operation with a current density of 100 mA cm^{-2}. Open circles: outer, Fe-rich scale; full circles: inner, Cr-rich scale.

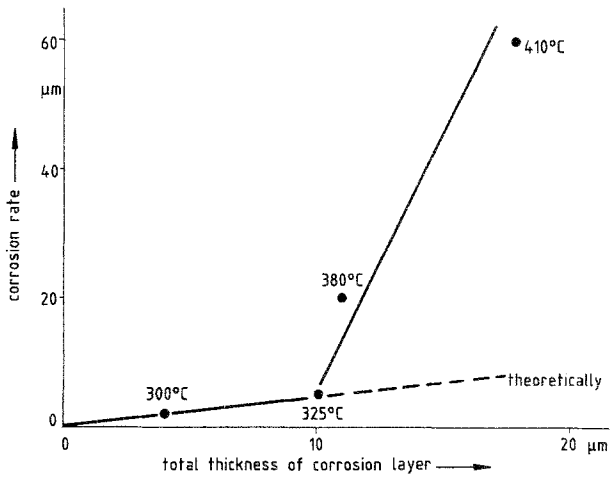

Fig. 6. Corrosion rate as a function of the total (Cr-rich plus Fe-rich) thickness of the anodic corrosion layer.

energy of 105 kJ mol^{-1}. The activation energy of the cathodic corrosion rate is essentially the same as in the anodic case, except at very high temperatures.

Figures 3 and 4 show examples of anodic corrosion layers at 325 and 410° C. There are two distinct scales to be discerned: an inner one, consisting of a chromium sulphide and an outer one, consisting mainly of an iron sulphide at lower temperature and an iron + chromium sulphide at higher temperatures. The thickness of these scales depends on the temperature as is shown in Fig. 5. Whereas the inner chromium sulphide layer increases continuously with temperature (70 kJ mol^{-1}), the outer iron sulphide-rich layer shows a discontinuity at medium temperatures. This behaviour becomes clearer when the total layer thickness (chromium + iron sulphide) is compared with the corrosion rate, as in Fig. 6. The theoretical behaviour could be calculated from Equations 2 and 3 and at lower temperatures there is good agreement with the experimental data. However, at higher temperatures, there is a steep increase in the corrosion rate. This indicates that in the high temperature range parts of the scale dissolve in the melt. Chemical analysis of the melt will be carried out in the course of further investigations, in order to gain more insight into this behaviour.

It should be noted that the corrosion rate without applied potential is at least a factor of 20 smaller than the values presented here. Also, we could identify alloys which show considerably smaller corrosion rates than those for the AISI 316 which served only as a 'model material' for the determination of fundamental behaviour.

4. Discussion

The mechanism of the corrosion during anodic operation is relatively straightforward. As in systems with sulphur vapour [13] at temperatures above 600° C, an inner chromium sulphide layer (Cr_2S_3 or Cr_3S_4) is formed, which acts as a barrier against rapid corrosion. Through this barrier iron and nickel ions are migrating, forming an outer layer with the corresponding composition. The influence of potential can be understood by assuming the following reaction for the iron corrosion:

$$2Fe + 3S_4^{2-} \longrightarrow 2FeS + 2S_5^{2-} + 2e^- \qquad (5)$$

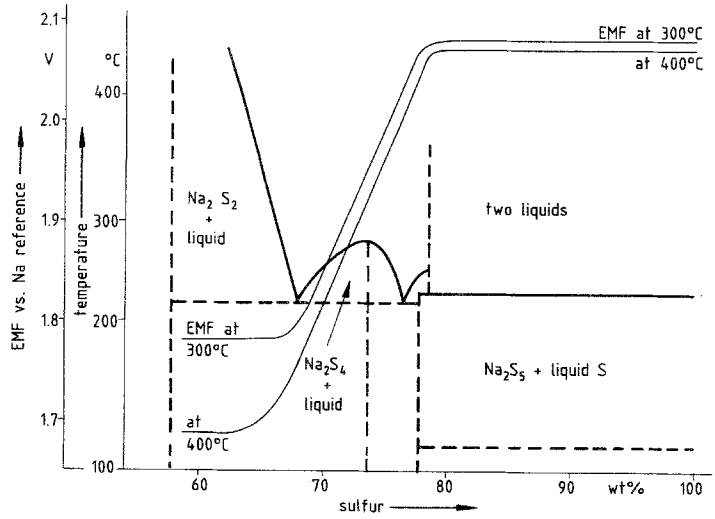

Fig. 7. Na_2S/S phase diagram and EMF at different temperatures (after [14]).

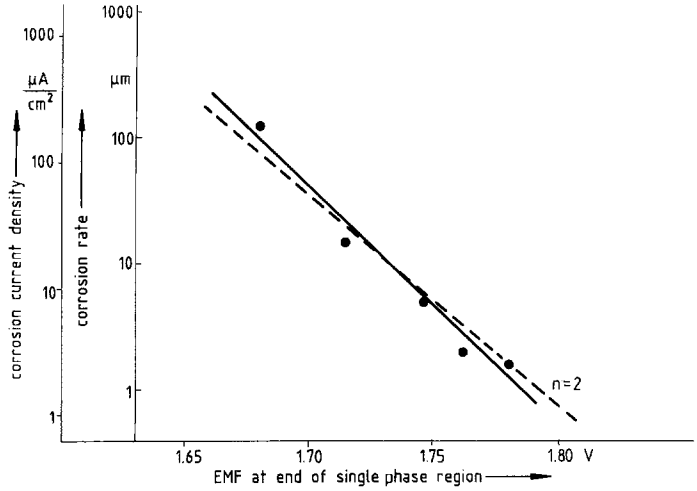

Fig. 8. Cathodic corrosion rate (and the corrosion current density calculated from the rate) as a function of the EMF at the end of the single-phase region (see Fig. 7). Dotted line: calculated for $n = 2$ ($RT/nF \simeq 60\,\text{mV}$ decade^{-1}).

Thus, by applying a potential, the sulphidation of iron can be accelerated. An increase in temperature may cause a corresponding increase in the rate constant of the iron migration through the chromium sulphide, thus accelerating the above reaction. As an activated process, this will depend exponentially on the temperature (Arrhenius), as was observed here.

During cathodic operation no corrosion scale was observed. Therefore the corrosion reaction must be quite different from Equation 5. As the cathodic potential is in the far cathodic region, sodium ions can be reduced [11]. Thus, the following reactions can be assumed:

$$\text{Fe} + 3\text{Na}^+ + 2e^- + \text{S}_4^{2-} \longrightarrow \text{Na}_3\text{FeS}_3 + 1/2\text{S}_2^{2-} \quad (6)$$

$$\text{Cr} + 3\text{Na}^+ + 2e^- + \text{S}_4^{2-} \longrightarrow \text{NaCrS}_2 + \text{Na}_2\text{S} + 1/2\text{S}_2^{2-} \quad (7)$$

The existence of Na_3FeS_3 and $NaCrS_2$ was shown in post-test examinations of Na/S cells [9, 15] (nothing has been published about the corresponding nickel compounds). As no corrosion scales could be found, these products obviously dissolve in the melt. In the (anodic) two-phase region the EMF changes very little with temperature, as can be seen from Fig. 7 (after [14]). However, in the (cathodic) one-phase region the EMF varies within broad limits. By plotting the corrosion rate vs the EMF at the end of the single-phase region (where the EMF becomes constant because of the transition into the two-phase region: Na_2S_2 + liquid). Fig. 8 is obtained.

It can be seen that a kind of Tafel line with a slope of about 60 mV decade^{-1} results. This value corresponds to a two-electron step ($n = 2$) with:

$$i \simeq \exp\left(-\frac{nF}{RT}U\right) \quad (8)$$

where i is the corrosion current and U the electrode potential. Therefore, the corrosion seems to be a potential-determined, two-electron process such as Reaction 6 and/or 7. Confirmation of this mechanism requires experiments carried out in complete Na/S cells where it could be shown that the corrosion rate is increased considerably with increasing depth discharge. This means that the corrosion rate depends on the electrode potential in the cathodic region (discharge direction). However, for a full understanding more investigations are necessary, e.g. potentiostatic operation mode and chemical analysis of the melt for corrosion products.

Acknowledgements

This work was sponsored in part by the Bundeministerium für Forschung und Technologie (reference ET-4496A). The author is grateful to Mr K. Reiss for experimental assistance and Dr S. Mennicke for valuable discussions.

References

[1] A. Wicker, G. Desplanches and H. Saisse, *Thin Solid Films* **83** (1981) 437.
[2] B. Hartmann, *J. Power Sources* **3** (1978) 227.
[3] R. R. Dubin, *Mat. Perform.* **20** (1981) 13.
[4] A. R. Tilley and M. L. Wright, 16 IECEC, Atlanta (1981) p. 841.
[5] D. S. Park and D. Chatterjii, *Thin Solid Films* **83** (1981) 429.
[6] B. Dunn, M. W. Breiter and D. S. Park, *J. Appl. Electrochem.* **11** (1981) 103.
[7] T. L. Markin, A. R. Junkinson, R. J. Bones and D. Teagle, *Power Sources Conf.* **7** (1979) 757.
[8] H. W. Wroblowa, R. P. Tischer, G. M. Crosbie and G. J. Tennenhouse, *Corros. Sci.* **26** (1986) 193, 371, 377.
[9] A. P. Brown and J. E. Battles, *J. Electrochem. Soc.* **133** (1986) 1321.
[10] A. P. Brown, *J. Electrochem. Soc.* **134** (1987) 1921.
[11] R. Knödler, *J. Electrochem. Soc.* **134** (1987) 1419.
[12] R. Knödler and S. Mennicke, *Electrochim. Acta* **28** (1983) 1033.
[13] S. K. Putatunda, *Mat. Sci. Engng* **82** (1986) 27.
[14] (a) N. K. Gupta and R. P. Tischer, *J. Electrochem. Soc.* **119** (1972) 1033; (b) D. G. Oei, *Inorg. Chem.* **12** (1973) 435.
[15] J. Battles, Posttest analysis of beta cells, EPRI-Report EM-4341. Dec. (1985).